ELSEVIER

Contents lists available at ScienceDirect

Bioresource Technology Reports

journal homepage: www.sciencedirect.com/journal/bioresource-technology-reports



Influence of nutrient medium supply rate and liquid recirculation regime on syngas biomethanation in thermophilic trickle-bed reactor

Florian Gabler a,b,*, George Cheng c, Leticia Pizzul b, Anna Schnürer c, Åke Nordberg a

- ^a Department of Energy and Technology, SLU, Box 7032, 750 07, Uppsala, Sweden
- ^b Department of Biorefinery and Energy, RISE, Box 7033, 750 07, Uppsala, Sweden
- ^c Department of Molecular Science, BioCenter SLU, Box 7015, 750 07, Uppsala, Sweden

ARTICLE INFO

Keywords: Biosyngas Digestate Hydraulic retention time Trickling Syntrophic acetate oxidation Methanothermobacter

ABSTRACT

Syngas biomethanation enables the use of recalcitrant biomass or waste for methane production. To reveal knowledge on the importance of nutrient medium supply rate (NMSR) and liquid recirculation regime, a thermophilic 5 L trickle-bed reactor was operated for 283 days. Efficient and stable operation with >99 % $\rm H_2$ and CO conversion rates was achieved at a minimum NMSR of 14 mL/($\rm L_{pbv}$ ·d) and 1 h gas retention time, yielding a maximum methane evolution rate (MER) of 4.3 L/($\rm L_{pbv}$ ·d). Reduced intermittent liquid recirculation resulted in lowered MERs (max. 3.4 L/($\rm L_{pbv}$ ·d)) with CO conversion more affected by low recirculation frequencies than $\rm H_2$ conversion. The microbial analysis revealed a similar microbial community structure across all experimental phases, dominated by *Methanothermobacter* in both liquid and carrier biofilm. CO was likely converted to methane and acetate, with syntrophic acetate-oxidizing bacteria metabolizing acetate to $\rm H_2$ and $\rm CO_2$, supporting efficient hydrogenotrophic methanogenesis.

1. Introduction

Covering the demand for biomethane (CH₄) within the near future is a central challenge of the European bioeconomy. To enhance CH₄ production without increasing pressure on the existing competition of energy vs. food, it is necessary to broaden the technological availability for biomethane production. Lignocellulosic-rich substrates (e.g., forestry residues) can currently not be used within traditional large-scale anaerobic digestion but can be thermochemically converted to syngas, which is typically comprised of hydrogen (H2), carbon monoxide (CO), carbon dioxide (CO2), and additional gases like nitrogen (N2) and CH4. Syngas serves not only as an energy source but also as an intermediate for producing high-value compounds such as methane, acetate, and liquid fuels (Neto et al., 2025). The process of syngas conversion into a useful energy carrier (CH₄) is attractive, as it allows the conversion of different types of low-degradable biomass, i.e., lignocellulosic material. This method improves the alignment with current gas infrastructure, thus promoting energy transport and storage (Ren et al., 2020). Syngas methanation can be achieved through either chemical or biological pathways: catalytic methanation via chemical processes under high temperature and pressure using metal catalysts such as nickel or iron, whereas biomethanation is a biological process mediated by

microorganisms of the domains Bacteria and Archaea (Ren et al., 2020). In contrast to catalytic methods, biomethanation operates under more moderate circumstances such as reduced pressures and temperatures, rendering it a more energy-efficient option (Grimalt-Alemany et al., 2017; Asimakopoulos et al., 2020). Furthermore, in contrast to chemical catalysts, microorganisms showed higher robustness to fluctuating gas load and pollutants, like tar and hydrogen sulfide (H₂S) (Grimalt-Alemany et al., 2017).

The dominant microorganisms that play a role in syngas biomethanation are acetogens, syntrophic acetate-oxidizing bacteria (SAOB), and methanogens (Paniagua et al., 2022). An overview about the most important biochemical reactions carried out by the different microbial groups is presented in Table 1. Hydrogenotrophic methanogens are also able to produce CH₄ from H₂ and CO₂, which are the same substrates that are utilized by homoacetogenic bacteria to produce acetate, resulting in a competitive relationship for H₂. A subgroup of hydrogenotrophic methanogens can directly convert CO to CH₄, while carboxydotrophic acetogens can convert it into acetate (Paniagua et al., 2022). Under thermophilic conditions, CO is more commonly converted into CO₂ by carboxydotrophic hydrogenogens via biological water-gas shift reaction (Sipma et al., 2003). However, the indirect route of CO conversion through acetate as an intermediate is usually more

^{*} Corresponding author at: Department of Energy and Technology, SLU, Box 7032, 750 07, Uppsala, Sweden. *E-mail address:* florian.gabler@slu.se (F. Gabler).

Table 1Biochemical reactions within syngas biomethanation mediated by different microbial groups.

Microbial group	Biochemical reaction	ΔG ⁰ [kJ/ mol]
Hydrogenotrophic methanogens	$CO_2 + 4H_2 \rightarrow CH_4 + 2H_2O$	-136
Homoacetogens	$2CO_2 + 4H_2 \rightarrow CH_3COOH +$	-105
	$2H_2O$	
Acetoclastic methanogens	$CH_3COOH \rightarrow CH_4 + CO_2$	-31
Syntrophic acetate-oxidizing	$CH_3COOH + 2H_2O \rightarrow 4H_2 +$	+95
bacteria	$2CO_2$	
Carboxydotrophic methanogens	$4\text{CO} + 2\text{H}_2\text{O} \rightarrow \text{CH}_4 + 3\text{CO}_2$	-212
Carboxydotrophic acetogens	$4CO + 2H_2O \rightarrow CH_3COOH +$	-176
	2CO ₂	
Carboxydotrophic hydrogenogens	$CO + H_2O \rightarrow CO_2 + H_2$	-20

predominant because of its preferable thermodynamics compared to direct conversion by carboxydotrophic hydrogenogens (Sancho Navarro et al., 2016).

Furthermore, syngas biomethanation is reported to show higher CH₄ productivity and greater CO tolerance at higher temperature (55–70 °C), combined with enhanced syntrophic acetate oxidation, leading to higher CH₄ yields as well as increased process stability (Andreides et al., 2022).

In general, CH₄ productivity is limited by temperature-dependent poor liquid-gas mass transfer and the slow kinetics of methanogens (Grimalt-Alemany et al., 2017). For the biomethanation of either syngas (H₂, CO₂, and CO) or only H₂ and CO₂, the trickle-bed reactor (TBR) is a feasible reactor to circumvent mass transfer restrictions (Paniagua et al., 2022). TBRs are gastight columns filled with microbe-covered carrier material, over which the liquid is trickled to supply nutrients to the microbial community. The carriers enhance the gas-liquid phase boundary interaction by offering the biofilm to develop on a large specific area relative to the reactor volume. Studies on biomethanation in TBR have illustrated the importance of various parameters, such as the choice of inoculum, temperature change, or the addition of external H₂ as reviewed in Feickert Fenske et al. (2023b). Moreover, to reach longterm process stability, it is essential that the nutrient supply contains sufficient nutrient concentrations to allow microbial activity and growth in TBRs. Substitutes for defined nutrient media, e.g., digestates, are increasingly utilized in recent studies (Aryal et al., 2021; Kamravamanesh et al., 2023; Ali et al., 2024; Goonesekera et al., 2024).

The hydraulic retention time (HRT) is usually used to describe the average time that the nutrient media liquid phase remains in the bioreactor before being discharged. A properly maintained HRT contributes to a stable pH, buffering capacity, as well as sufficient nutrient supply, which is the basis for effective syngas biomethanation (Kamravamanesh et al., 2023). Furthermore, the HRT of the nutrient liquid in the TBR is of importance for assessing economic feasibility as handling large volumes of nutrient media is associated with high operational costs. For TBR syngas biomethanation using digestate as a nutrient medium, HRTs between 5 and 31.5 d are documented (Andreides et al., 2022; Cheng et al., 2022; Ali et al., 2024; Goonesekera et al., 2024; Gabler et al., 2025) but have so far not been systematically investigated for TBR syngas biomethanation. Lowering nutrient feeding can influence the biological syngas conversion and CH4 productivity and, thus, the techno-economic characteristics of the process. Finding a well-balanced supply of nutrient media is therefore essential for an efficient operation of syngas biomethanation. Closely connected to the HRT is the nutrient medium supply rate (NMSR), which takes the liquid reservoir volume of the TBR setup into consideration, allowing comparability among different TBR biomethanation studies.

The liquid recirculation regime relates to different approaches, which include frequency, duration, and the liquid volume flow rate, and does not only provide essential nutrients to the biofilm and removes inhibitory metabolites but also creates a liquid barrier for efficient gasliquid mass transfer on the carrier (Sieborg et al., 2021). Studies about

TBR syngas biomethanation were performed both with continuous recirculation (Asimakopoulos et al., 2021; Andreides et al., 2022; Ali et al., 2024; Goonesekera et al., 2024) and semi-continuous, i.e., intermittent recirculation (Aryal et al., 2021; Cheng et al., 2022; Bilgic et al., 2025; Gabler et al., 2025). However, the intensive liquid recirculation is reported to negatively affect MER and H2 conversion rates in TBR biomethanation of H₂ and CO₂ (Ashraf et al., 2021; Sieborg et al., 2021). A decreasing recirculation is suspected to allow higher gas loads to the TBR, resulting in higher methane productivity (Burkhardt et al., 2015). However, to date, there are only two studies that have systematically assessed this research question. Ashraf et al. (2021) were testing different supply methods, i.e., flushing, flooding, and continuous recirculation within a 0.5 L TBR for the biomethanation of H2 and CO2. It was concluded that applying a large flow of liquid disrupted the gas-liquid mass transfer. In line, Sieborg et al. (2021) assessed the influence of different recirculation regimes for biomethanation of H2 and CO in mesophilic fed-batch operated 1.5 L TBRs, observing a significant enhancement of H₂ consumption rate when recirculation was applied once per week instead of once per day. For the biomethanation of syngas, this parameter has not been evaluated, and the liquid recirculation has been operated in continuous mode in most studies (Asimakopoulos et al., 2020; Andreides et al., 2022; Goonesekera et al., 2024). It can be hypothesized that insufficient recirculation can impair CO and H2 conversion due to localized inhibition of the prevailing microbial groups.

The objective of this study was to assess the influence of the NMSR and the liquid recirculation regime concerning the $\rm H_2$ and CO conversion and the CH₄ production of syngas biomethanation in a thermophilic TBR using diluted manure-based digestate as the sole nutrient medium. To our knowledge, this study presents the first systematic assessment of the recirculation regime for syngas biomethanation using a TBR, assessing the recirculation frequency in combination with the recirculation duration. An additional aim of the study was to examine microbial community development with an emphasis on possible variations based on the applied changes in process parameters.

2. Materials and methods

2.1. TBR setup and nutrient media

The reactor setup used in this study is described in detail in a previous article (Gabler et al., 2025) and presented in Fig. S1, Supplementary Material (SM). Briefly, the TBR was a stainless-steel column with a packed bed volume of 5 L and a liquid volume of 1 L, and was operated at a temperature of 56 \pm 1 $^{\circ}$ C. The TBR used in the present study had been continuously operated with digestate as the sole nutrient source in a previous study for 382 days, mainly maintaining an HRT of 7.5 d. For biofilm growth, high-density polyethylene carrier material AnoxKaldnes K1 500 (10 mm diameter, surface area 500 m²/m³, density 1.2 g/m³) was used. The utilized syngas was an artificial mixture supplied by Air Liquide (Paris, France) with 40 % H₂, 30 % CO, 20 % CO₂ and 10 % N2 to mimic an industrial syngas mixture according to the GobiGas project, utilizing forestry biomass as gasification substrate (Larsson et al., 2019). The syngas load was controlled by a mass flow regulator (MFR, Aalborg DPC17; Orangeburg, US) and was continuously added through a port between the liquid reservoir and the packed bed (Fig. S1; SM) to meet the liquid coming from the top, thus operating in a counter-current manner. No significant overpressure was applied to the TBR. The product gas was collected above the packed bed at the top of the reactor. Its volume was measured using a drum meter (TG 0.5; Ritter, Germany) after it passed through a condensed water trap. It then passed another condensed trap and entered the gas storage. Using an ETG MCA 100 Syn Biogas Multigas Analyzer (ETG Risorse e Tecnologia s.r.l., Chivasso, Italy), the composition of the produced gas was analyzed for CH₄, CO₂, CO, O₂, and H₂ in batches of around 3 L from the gas storage, resulting in semi-continuous measurements every 40 to 50 min.

The digestate used as a nutrient medium was collected from a

mesophilic biogas reactor (SLU, Lövsta, Uppsala, Sweden), which primarily operates with manure from pigs and cows. Batches of approximately 60 L were collected at the beginning of the study (day 382) and on day 574 for subsequent storage at 2 °C. Before application to the reactor, the digestate was filtered through a mesh column (4/2/1 mm), diluted with 50 % tap water to reduce the risk of clogging in the reactor, and subsequently stored at 6–8 °C before being pumped into the reactor. Diluted digestate was pumped into the liquid reservoir using peristaltic pumps (WMC, 200 Series, Southwick, UK), depending on operational conditions within the corresponding periods (Fig. 1). Table 2 shows the initial characterization of the diluted digestate used as the nutrient medium. To maintain a constant liquid volume in the TBR, the process liquid was manually sampled every 3–4 days from the liquid reservoir (Fig. S1, SM).

2.2. Key performance indicators

The average inflow-based hydraulic retention time (HRT) of the nutrient media was calculated based on the addition of nutrient medium V_M (L/d) to the reactor and the total liquid volume V_L in the reactor (1 L), as follows:

$$HRT = \frac{V_L}{V_M} \tag{1}$$

To allow comparability of the nutrient addition strategies among the literature, the Nutrient Medium Supply Rate (NMSR) [mL/(Lpbv·d)] was calculated by dividing the addition rate of fresh nutrient medium (mL/d) by the total packed bed volume (Vpbv) of the TBR (Eq. 2).

$$NMSR = \frac{V_M}{V_{pbv}} / 1000 \tag{2}$$

To analyze reactor performance concerning CH₄ production, the Methane Evolution Rate (MER) was calculated as shown in Eq. 3. Here, F_{out} (NL/(L_{pbv}·d)) is defined as the total normalized product gas flow rate (1013.15 mbar, 273.15 K), and c_{CH4} is the CH₄ composition in the product gas.

$$MER = F_{out} * c_{CH4}$$
 (3)

To follow the conversion of H_2 and CO, the conversion rate (%) of each component was calculated according to Eq. 4, where F_i in is the normalized flow rate of the specific gas compartment in the inlet gas (NL/(L_{pbv}·d)) and F_i out is the normalized flowrate of it in the product gas at the outlet of the TBR.

$$conversion rate = \frac{F_i in - F_i out}{F_i in} *100$$
 (4)

 Table 2

 Initial characteristics of (diluted) digestate used as nutrient medium.

Parameter	Unit	Diluted digestate
рН	_	8.5
Alkalinity	mg CaCO ₃ /L	7264
Volatile Fatty Acids	g/L	0.07
Ammonium	mg/L	850
Sulphate	mg/L	282
Phosphate	mg/L	70
Sodium*	mg/L	206
Potassium*	mg/L	1510
Calcium*	mg/L	146
Magnesium*	mg/L	51
Iron*	mg/L	12
Cobalt*	μg/L	15
Copper*	μg/L	1180
Molybdenum*	μg/L	63
Nickel*	μg/L	94
Zinc*	$\mu g/L$	3060

* Analysis of Na, K, Ca, Mg, Fe, Co, Cu, Mo, Ni, and Zn was externally conducted by the accredited ALS Scandinavia AB according to SS-EN ISO 17294-2:2016 and SS-EN ISO 11885:2009 on day 525 (with an error margin of 10–15 %).

The inflow-based Gas Retention Time (GRT) was defined as the average time for the gas to stay in the packed bed volume without conversion of the gases according to Eq. 5, where V_{pbv} is the active packed bed reactor volume (mL), and F_{in} is the total normalized inflowing gas load (mL/h).

$$GRT = \frac{V_{pb\nu}}{F_{in}} \tag{5}$$

2.3. Process operation

The present study follows a previous study where diluted manure-based digestate was utilized in the same TBR setup at an NMSR of 27 mL/(L_{pbv} ·d), resulting in MERs of up to 4.5 L/(L_{pbv} ·d) and high H₂ and CO conversion rates above 95 %, dominated by *Methanothermobacter* in both TBR liquid and carrier biofilm (Gabler et al., 2025).

The major operational guideline of this study was to maintain similar high $\rm H_2$ and CO conversion rates (>95 %) throughout the experiment. The adjustments of process parameters, such as syngas loads or nutrient supply, were based on the development of the conversion rates, accompanied by changes in MER.

The effect of the nutrient medium supply rate (NMSR) was evaluated during the first 182 days of the study (from day 382 to day 564, considering the entire reactor operation time). The NMSR was adjusted

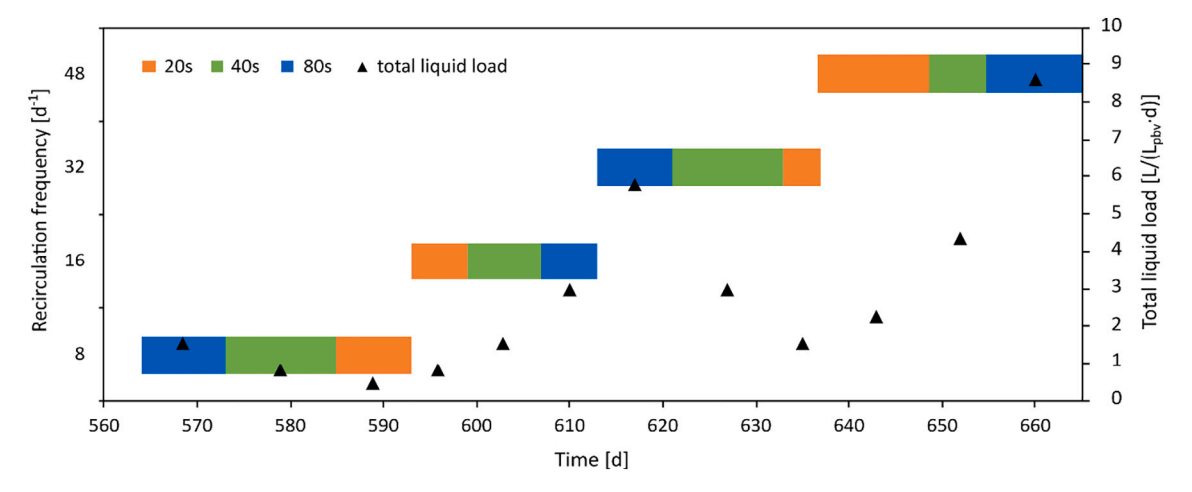


Fig. 1. Operational periods of the assessment of the liquid recirculation regimes with varying recirculation frequencies (8, 16, 32, and 48 d⁻¹) and recirculation duration (80s, 40s, and 20s) resulting in different total liquid loads (0.3–8.5 L/(L_{pbv} -d) between day 564 and 665.

as described in Table 3 and the liquid recirculation regime was kept constant (20 s recirculation duration at a frequency of $144~d^{-1}$, total average flow of 40~L/h, nutrient liquid load of $6.4~L/(L_{pbv}\cdot d)$). The liquid recirculation regime was investigated between day 564 and day 665, by periodically increasing the recirculation frequency $[d^{-1}]$, i.e., the number of trickling occasions, combined with varying recirculation duration (20s, 40s, and 80s) according to Fig. 1. The applied total liquid loads ranged between 0.4 and 8.5 $L/(L_{pbv}\cdot d)$. The NMSR was kept constant at $14~mL/(L_{pbv}\cdot d)$, resulting in a corresponding HRT of 14.5~d.

2.4. Sampling and chemical analysis

The removed process liquid from the liquid reservoir was used for chemical and microbial analyses. Carriers from the TBRs were sampled on two occasions, on day 564 and day 665 from the valves at the top, middle and bottom of the reactor (Fig. S1, SM) while flushing with N_2 (5 mL/min). Removed carriers were replaced by clean ones.

Analysis of alkalinity, pH, macronutrient concentrations (NH $_{\tau}^{+}$, SO $_{\tau}^{2-}$, PO $_{\tau}^{3}$) in the liquid phase, and hydrogen sulfide (H $_{2}$ S) in the product gas were performed as in a previous study (Gabler et al., 2025). Volatile fatty acids (VFA) were analyzed by high-performance liquid chromatography, Shimadzu 2050 Series, equipped with an ion exclusion column (Rezex ROA - Organic Acid H+, 300 \times 7.80 mm, Phenomenex) and detected by a RID detector. The mobile phase used was 5 mM H $_{2}$ SO $_{2}$ with a flow rate of 0.6 mL/min. Samples (700 μ L) were mixed with 70 μ L of H $_{2}$ SO $_{4}$ (5 M), centrifuged (14.000 RCF, 15 min), and filtered through a 0.2 μ m syringe filter into an HPLC glass vial. Micronutrients (Na, K, Ca, Mg) and trace elements (Fe, Co, Cu, Mo, Ni, Zn) were analyzed externally by the accredited ALS Scandinavia AB using ICP-AES and ICP-SMFS.

2.5. Microbial sequencing and analysis

The DNA extraction was completed on 2 mL of liquid sample using FastDNA Spin Kit for Soil (MP Biomedicals, Illkirch-Graffenstaden, France) following the manufacturer's instructions. Modifications were made in step 7 (10 min centrifugation at 14000 RCF) and step 9 (10 min of matrix settling). In addition, an additional cleaning step between steps 11 and 12 was applied to remove PCR-inhibiting components, as suggested by the manufacturer, with the procedure for humic acid removal for soil samples (MP Biomedicals, LLC). Additional steps were taken for carrier samples as described in Gabler et al. (2025). The carrier samples were extracted in quadruplicate to collect enough material from the biofilm on the carriers. Sequencing libraries were prepared and generated by Novogene Europe, Munich, Germany, using Illumina MiSeq targeting 16 s rRNA as described previously (Westerholm et al., 2018). The paired-end reads were filtered based on quality and trimmed reads to 250 bp. Downstream processing of the reads was completed using Division Amplicon Denoising Algorithm2 (DADA2, v. 1.32.0) in RStudio running R v.4.4.1 as previously described in Westerholm et al. (2018), truncating forward and reverse reads at positions 180 and 200, respectively. The sequences for the quadruplet carrier samples were merged for downstream analysis. The SILVA reference database v. 138 was used for microbial classification. Phyloseq v1.48.0 was used to

Table 3Applied nutrient medium supply rates and corresponding hydraulic retention times between days 382 and 564.

Duration	Nutrient medium supply rate	Hydraulic retention time	
[d]	$[mL/(L_{pbv}\cdot d)]$	[d]	
382-410	22	8.9	
410-441	19	10.5	
441-472	14	14	
472-522	11	18	
522-564	14	14.5	

organize the sequence data. Weighted principal coordinate analysis (PCoA) was calculated using the UniFrac method based on the neighborjoining phylogenetic tree generated with DECIPHER (v3.0.0) and phangorn (v.2.12.1) (GTR model). To determine the correlation of process performance with each principal coordinate axis, parameter vectors (H₂ conversion, CO conversion, and syngas load) were fit to the PCoA ordination using the "envfit" function from vegan (v. 2.6.6.1). For the archaeal and bacterial PCoA plots, two outliers (day 606 and 627) were removed due to operational and monitoring malfunction. ASV species similarity was determined using the Basic Local Alignment Search Tool (BLAST) algorithm provided by the National Center for Biotechnology Information (NCBI) was used. Raw sequence data have been deposited in the NCBI.

3. Results

The results in this section are divided into three parts: the effect of the nutrient medium supply rate (NMSR) at different HRTs, the effect of the liquid recirculation regime, and the microbial community development.

As a result of the major operational guideline to maintain high $\rm H_2$ and CO conversion rates, no periods of VFA accumulation (< 0.3 g/L) were observed during the entire operation of 283 days (Fig. S2d and S3d, SM). The potential contribution of CH₄ in the diluted digestate used as a nutrient medium was negligible. In the present study, both the TBR setup and the nutrient medium were identical to a previous study (Gabler et al., 2025), where the maximum daily CH₄ production from the digestate, based on the highest supply rate (NMSR 27 mL/(Lpbv·d)) and residual methane potential (20 ml/g VS), would only result in ca. 2 mL CH₄/d when the daily syngas-derived CH₄ production was up to 22 L.

3.1. Nutrient medium supply rate

The nutrient medium supply rate (NMSR) was decreased stepwise as presented in Table 3, starting with 22 mL/(Lpbv·d) on day 382, reaching the lowest assessed NMSR (11 mL/(L_{pbv} ·d); HRT 18.9 d) on day 472. From the start until day 494, the syngas load was kept constant at a range of 24–25 $L/(L_{pbv}\cdot d)$ corresponding to GRT 1 h, maintaining full conversion of H2 and CO (Fig. 2b). Due to the temporary malfunction of the drum meter that was used to measure the volume of the product gas, the methane evolution rate (MER) achieved were assessed based on the observed conversion rates of H₂ and CO and the applied syngas load (Fig. 2a). The resulting calculated MER in this period was approximately 4.3 L/(L_{pbv}·d). During the NMSR periods 19, 14, and 11 mL/(L_{pbv}·d) (HRT 8.9, 10.5, and 14 d), H2 and CO conversion rates were very high (>99 %). Throughout the study, the pH in the process liquid remained stable between 7.5 and 8, with a temporary increase to 8.3 during the standby period. It returned to normal levels without pH control after syngas application was continued. During the whole operation, alkalinity remained sufficient, ranging from 4000 to 5500 mg CaCO₃/L (Fig. S2c and S3c, SM).

Between operation days 494 and 503 (at NMSR 11 mL/(L_{pbv} ·d), the operation was set to a standby mode for instrument maintenance and repair. The TBR received a low inflow of pure nitrogen (no syngas was supplied) and the temperature and NMSR were kept constant. This 9-day-long standby period subsequently affected H_2 and CO conversion rates and CH_4 productivity. After a stepwise increase of the syngas loads to the previous level of 24 L/(L_{pbv} ·d) (GRT 1 h) on day 516, the conversion for H_2 and CO reached 98 % and 97 %, respectively. To continue recovering conversion rates of H_2 and CO to previous levels above 99 %, the syngas load was decreased to ca. 22 L/(L_{pbv} ·d), corresponding to GRT 1.1 h, from 517 onwards. However, the H_2 and CO conversion rates did not reach the previous levels, even with this reduced syngas load compared to the previous periods before day 494. Based on the hypothesis that lower H_2 and CO conversion rates and CH_4 productivity

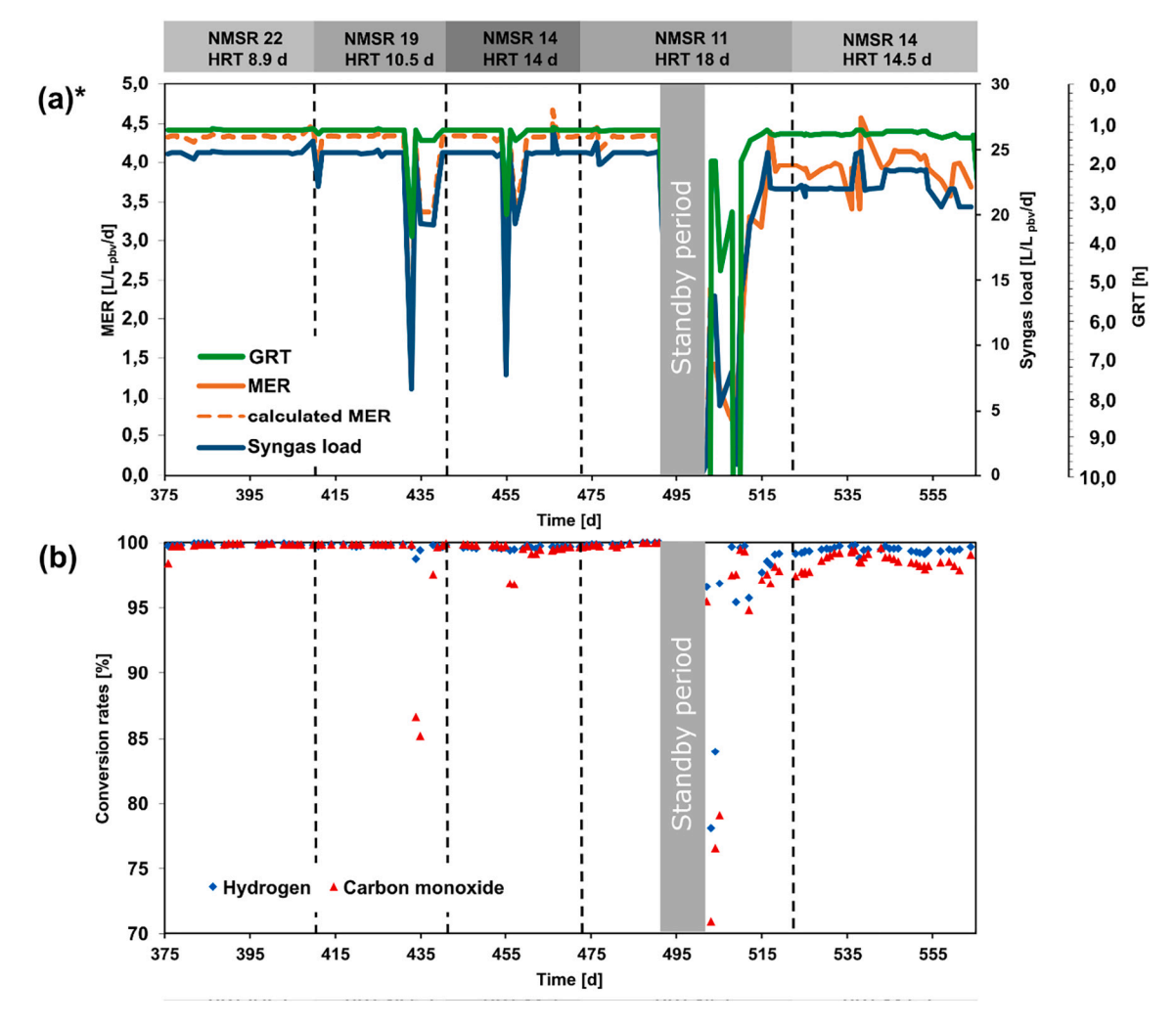


Fig. 2. Evaluation of the nutrient media supply rate (NMSR) between day 382 and 564: (a) Development of syngas load and (calculated) Methane Evolution Rate (MER)*, (b) H₂ and CO conversion rates. Data between day 0 and 381 is presented in a previous article (Gabler et al., 2025). *Up to day 500, the volumetric measurements of the product gas were not working correctly; therefore, the MER was calculated based on syngas inflow and achieved syngas conversion rates. Two major declines in the applied syngas load on days 433 and 455 were due to mechanical problems with the pressure control unit at the top of the syngas cylinder.

were related to the NMSR of 11 mL/(L_{pbv} ·d), which was low in comparison to other similar studies under thermophilic conditions (Andreides et al., 2022; Ali et al., 2024; Goonesekera et al., 2024; Gabler et al., 2025), and as no obvious shortages of macronutrients in the TBR liquid were observed, the NMSR was increased back to 14 mL/(L_{pbv} ·d). This resulted in a decreased average HRT of 14.5 d, which was kept until the end of the experiment. By increasing the NMSR, H_2 and CO conversion rates slowly improved to levels above 99 % between days 525 and 535. To further maximize MERs and maintain high conversion rates, the syngas load was increased from 21.9 to 23.3 $L/(L_{pbv}$ ·d) on day 543. However, this resulted in slowly decreasing conversion rates for H_2 (99 %) and CO (98 %).

3.2. Recirculation regime

After carrier sampling on day 564, the liquid recirculation sub-trial started on day 564 by reducing the recirculation frequency from 144 d^{-1} to 8 d^{-1} accompanied by a 4-fold increase of the recirculation duration from 20 s to 80 s (Fig. 1). The syngas flow subsequentially started in a reduced manner at 10 L/(Lpbv·d) (GRT 1.8 h) and was stepwise increased to 19 L/(Lpbv·d) (GRT 1.3 h) on day 572 resulting in a maximum MER of ca. 3.4 L/(Lpbv·d) (Fig. 3a). During this period until day 573, decreasing CO conversion rates were observed (98 to 96 %). At a recirculation duration of 40 s in the next period (until day 584), the

conversion rates remained stable at 99 % and > 96 % for H₂ and CO, respectively. However, when reducing the duration to 20 s with a frequency of 8 d⁻¹, a significant drop in the CO conversion rates to 90 % was observed, which might be rather associated with a rapid syngas load increase from 14 to 19 $L/(L_{pbv}\cdot d)$ between day 586 and 588 than with the change of the recirculation regime. At syngas loads of 19 L/(Lpby·d) (GRT 1.2-1.3 h), the CO conversion rates did not reach the previously observed high levels and levelled off at around 93 %. This trend continued during the next period with a 20 s recirculation duration and an increased recirculation frequency of 16 d^{-1} (days 593 to 599). However, CO conversion improved from day 605 onwards when a recirculation duration of 40 s at a frequency of 16 d⁻¹ was applied, reaching H₂ and CO conversion rates of >96 %. These rates remained stable after a further increase of the recirculation duration to 80 s (day 608). After day 613, when the recirculation frequency was increased to $32 d^{-1}$, conversion rates for H₂ were > 99 % and for CO were 97–98 %. Between days 630 and 665, at a frequency of 48 d⁻¹ (regardless of the recirculation duration), the conversion rates were constant in the range of 99 % for H2 and 96 % for CO. As for the NMSR sub-trial, no VFA accumulation was observed due to the applied major guideline to maintain high H₂ and CO conversion rates (Fig. S3d, SM). Moreover, the nutrient status reflected in Fig. S3a and b (SM) did not indicate any limitation in this part of the study.

To further evaluate the influence of liquid recirculation, the

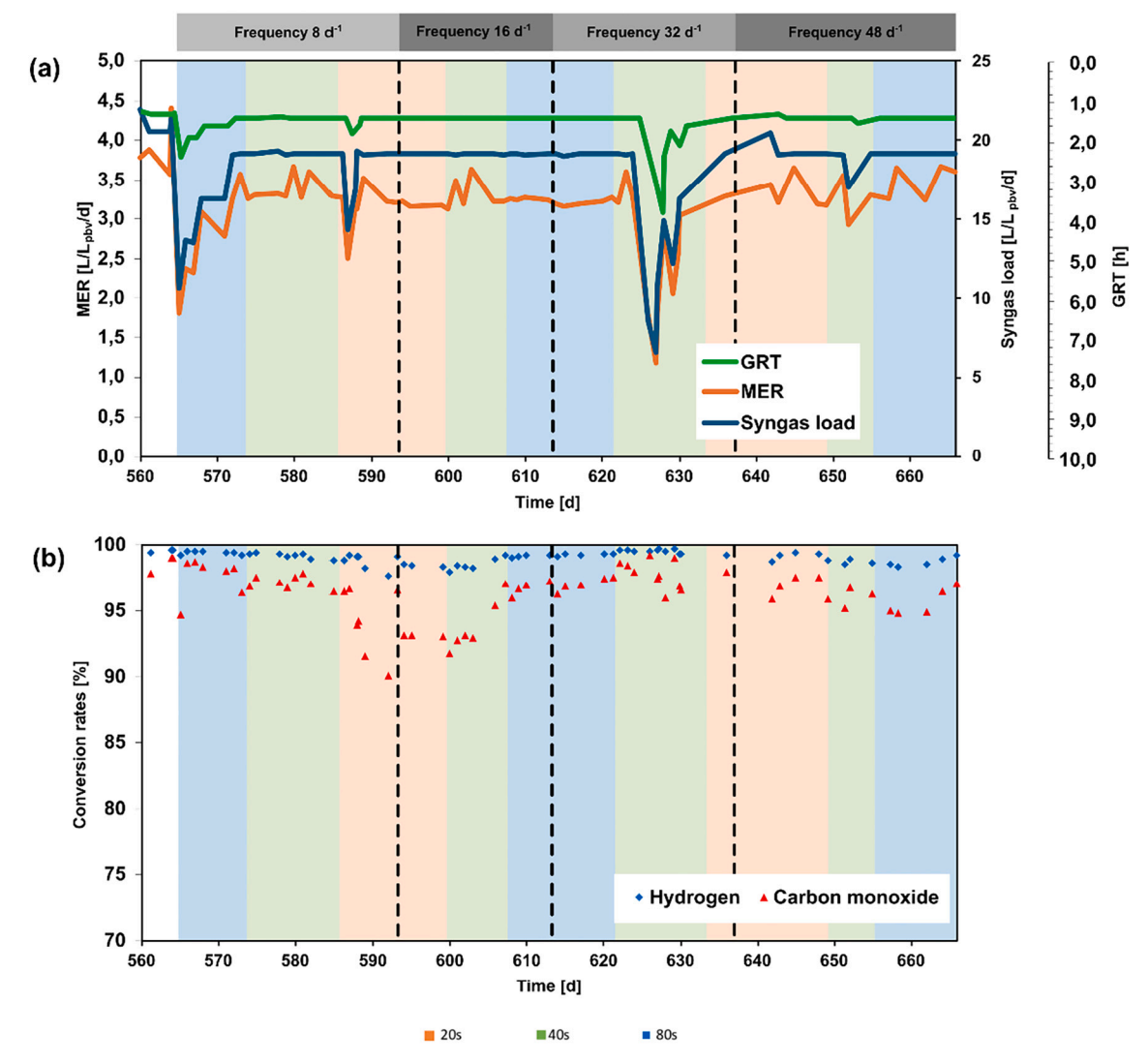


Fig. 3. Liquid recirculation assessment under different trickling frequencies and trickling durations according to Fig. 2 between day 564 and 665: (a) Development of syngas load and Methane Evolution Rate (MER), (b) H₂ and CO conversion rates.

concentrations of H_2 and CO in the product gas were observed at a higher resolution (24 h) during selected operation days (573, 579, and 590), under a recirculation frequency of 8 d $^{-1}$ (Fig. 4). The variation in CO concentration in the product gas showed 8 peaks within 24 h, a pattern that clearly corresponded to the recirculation frequency (Fig. 4). Each trickling occasion resulted in an increase in CO concentration in the product gas from ca. 1.2 % to 1.6 %. The recirculation duration, however, did not have any influence on the overall CO conversion (Fig. 4). The concentration of H_2 was around 0.4 % and was not affected by the recirculation occasions or recirculation durations, except for the long duration (80 s) where the 8 peaks-pattern observed for CO was also detected for H_2 , although the difference between peaks and valleys were lower for H_2 (ca. 0.1 %) compared to CO conversion (ca. 0.4 %).

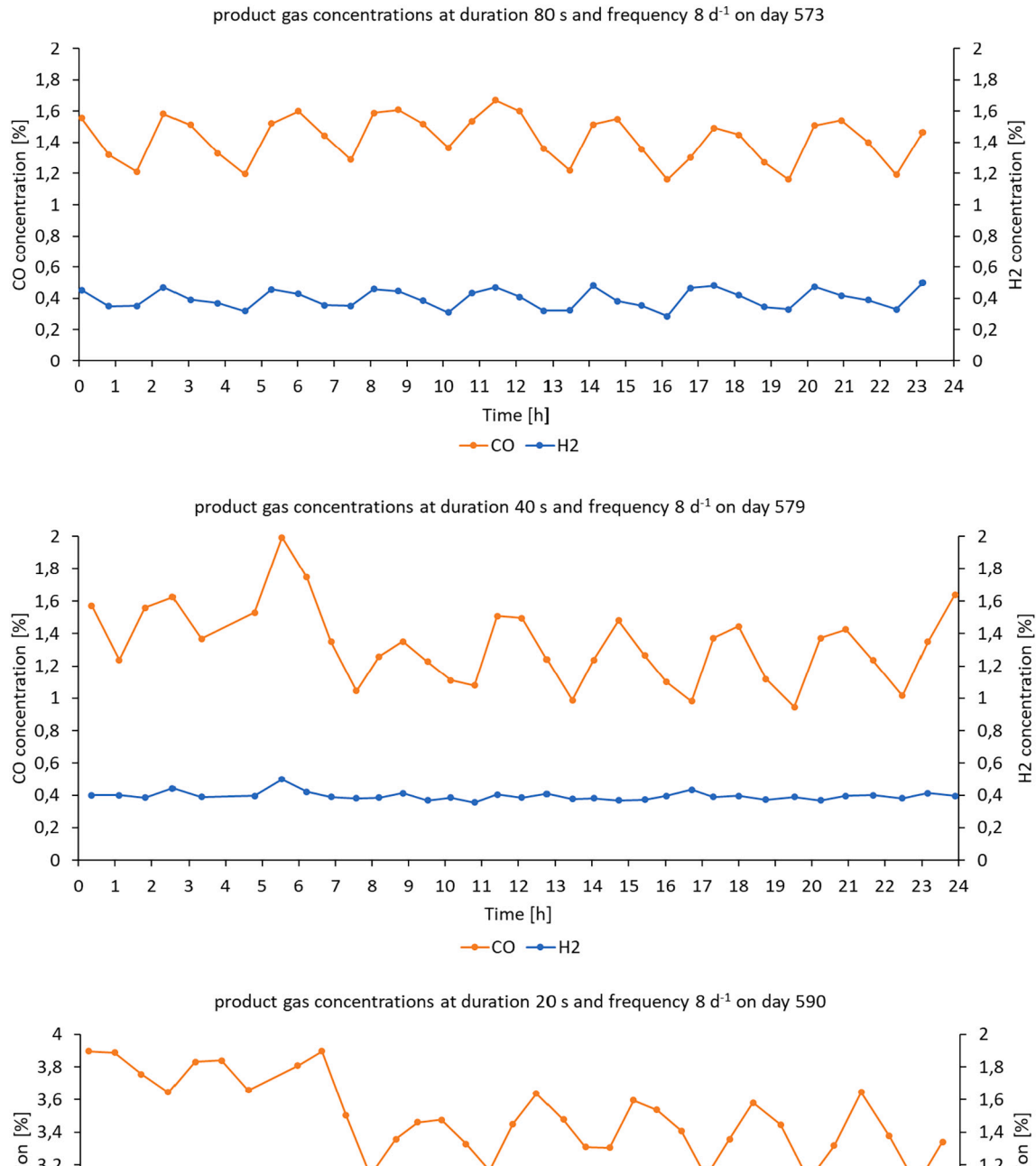
3.3. Microbial community development

PCoAs were performed to identify correlations between microbial community and TBR performance parameters during the different operational period of both sub-trials. One PCoA illustrates that the microbial community differed between the nutrient medium and the TBR (liquid phase and carrier biofilm) (Fig. S4, SM). Looking at the taxonomic affiliation, the overall microbial community showed only small changes during the changes of NSMRs and liquid recirculation regime,

both in the TBR liquid and on the carriers (Figs. S5-S8, SM). In another PCoA, Fig. 5 shows some separation of both the archaeal (Fig. 5a) and the bacterial (Fig. 5b) communities in the liquid and on the carriers during the different operational periods, but no strong positive correlation was found to syngas load or to the $\rm H_2$ or CO conversion rates. These results demonstrate the robustness of the microbial community in the process for operational changes and the low impact of the complex nutrient source. Considering the most abundant microbes (>1 % in relative abundance (RA)), 28 amplicon sequence variances (ASVs) in the NMSR period and 27 ASVs in the liquid recirculation regime period represent approximately 90 % of the community. A more detailed presentation of ASVs showing presence persisting through the entirety of each experimental phase is shown below.

3.3.1. Archaea

The archaeal community consisted primarily of an ASV belonging to the genus Methanothermobacter. This ASV was the dominating methanogen in the liquid phase throughout both sub-trials, representing 33–51 % of the total community and > 75 % of the archaea (Figs. S5 and S7, SM). NCBI analysis of the ASV assigned the closest relative as *Methanothermobacter thermautotrophicus*. The same ASV also dominated on the carriers, during the NMSR trial and in similar RA as in the liquid (day 564) and recirculation regime (day 665, 33–40 % RA), with very



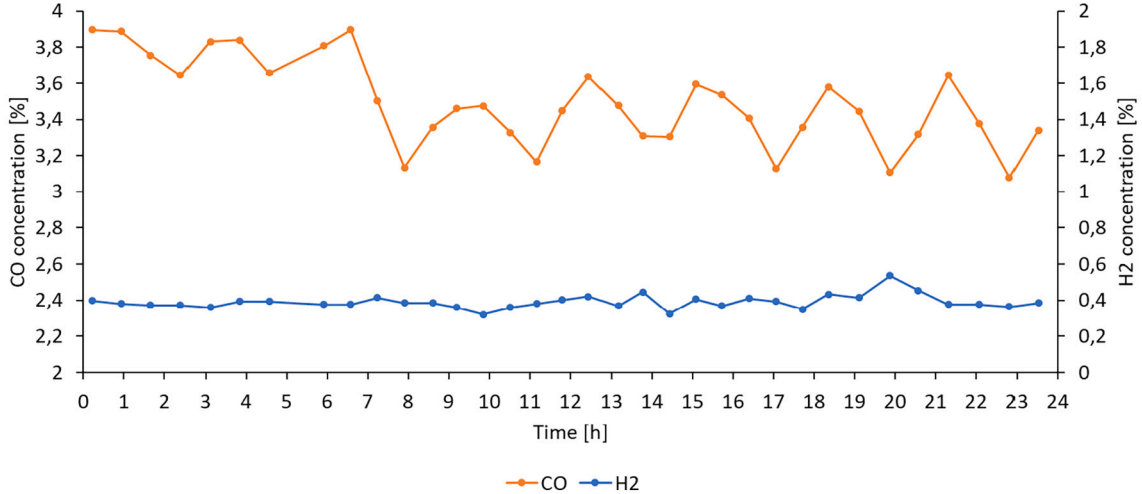


Fig. 4. Influence of recirculation occasions on the H_2 and CO conversion rates within 24 h (presented as H_2 and CO concentrations in the product gas) at different recirculation durations (80s, 40s, and 20s) at a recirculation frequency of $8d^{-1}$.

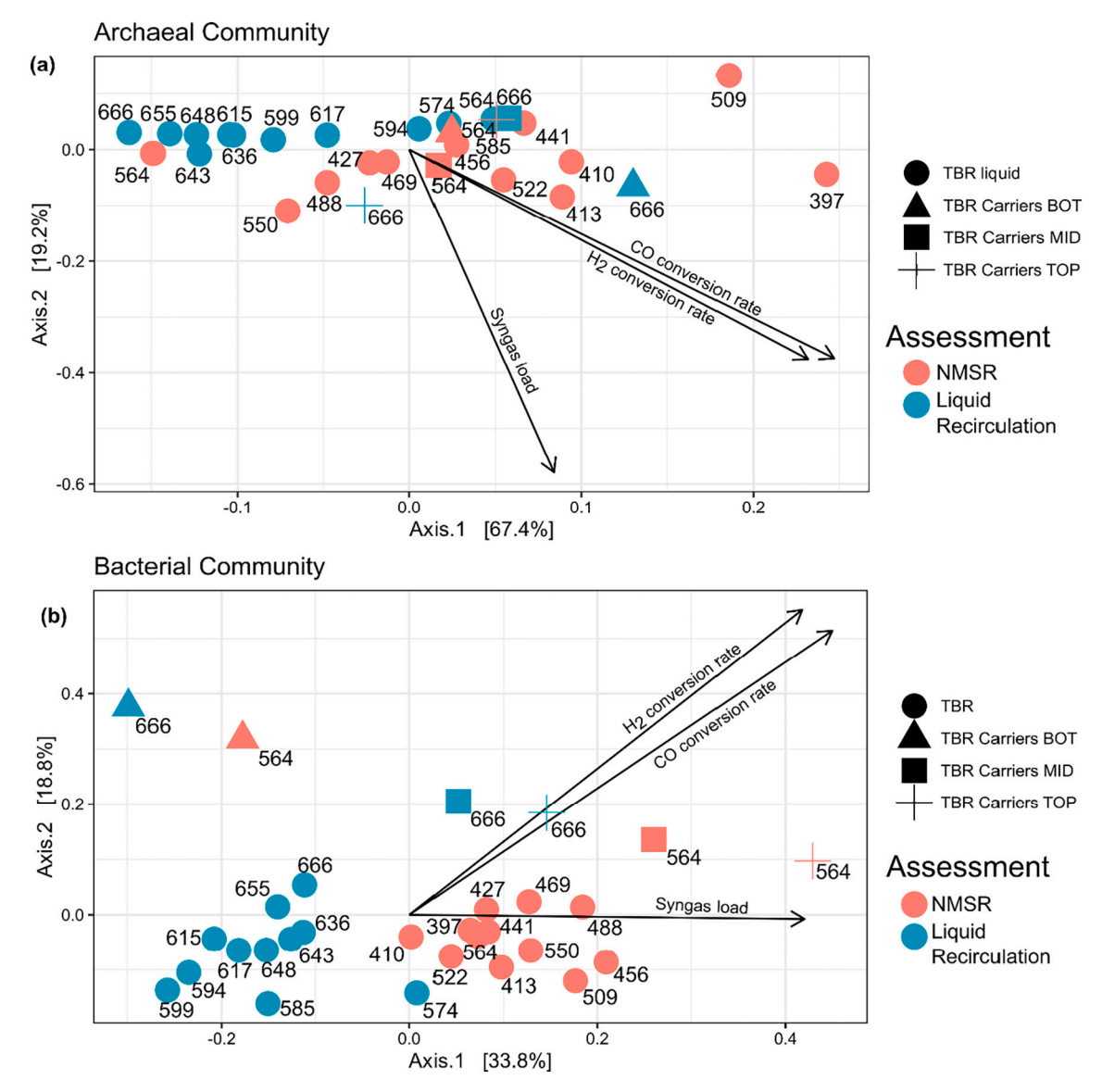


Fig. 5. Principal coordinate analysis (PCoA) plots of (a) the archaeal community and (b) the bacterial community in the TBR liquid and on the carriers using UniFrac. Indicators of process performance associated with changes in microbial community structure are plotted as vectors, where the direction and length indicate the contribution of the variable to the principial coordinates. The numbers indicate the day of operation in both conducted sub-trials (NMSR and Liquid Recirculation).

small differences between top or bottom of the TBR (Figs. S5 and S7, SM). Additional methanogens, both hydrogenotrophic, acetoclastic, and methylotrophic methanogens, were detected at very low RA (Figs. S5 and S7, SM). Of the low-abundant methanogens, one was identified at slightly higher RA, both in the liquid phase (mainly during the NMSR sub-trial) and on the carriers. This ASV was identified as Methanobacterium formicicum (Table 4). In addition, Methanosarcina, closely related to Methanosarcina thermophila (100 % similarity), showed a comparably higher RA on the top carriers during the NMSR sub-trial (Figs. S5 and S7, SM, Table 4). In the PCoA plot presented in Fig. 5a, the archaeal community clusters close to the center along principal coordinate 1 (67 % variance). Samples from the NMSR sub-trial show a broader spread compared to the liquid recirculation sub-trial. The vectors indicated that the CO and H2 conversion rates are more associated with the positive direction of principal coordinate 1, while syngas load is more associated with principal component 2 (19 % variance).

3.3.2. Bacteria

The bacterial community composition in the TBR liquid did not show any major differences throughout the experimental period including both sub-trials (Figs. S6 and S8, SM). ASVs, present throughout both subtrials, were represented by Aggregatilineales, D8A-2, Desulfitobacteriaceae, DTU014, Haloplasma, Hydrothermae, MBA03, Symbiobacterium, Syntrophaceticus, and W5 (Figs. S6 and S8, SM). Caldicoprobacter was present in the NMSR sub-trial but decreased in RA below 1 % after day 564 (during the liquid recirculation sub-trial) (Figs. S6 and S8, SM). A similar trend was seen for Tepidanerobacter. In contrast, Acetomicrobium and Coprothermobacter increased in abundance after 456 and 594 days, respectively. Tepidimicrobium was also more prevalent after day 574 (Fig. S8, SM). In the PCoA plot presented in Fig. 5b, the bacterial community shows a clearer separation between NMSR and liquid recirculation sub-trial than the archaeal community (Fig. 5a), with liquid recirculation samples clustering to the negative side of principal coordinate 1 and NMSR samples positioned more toward the positive side aligning strongly with syngas load and conversion rates vectors. Analysis of the bacterial community on the carrier at different positions of the TBR indicated some differences, such as Syntrophaceticus and Tepidanaerobacter being more abundant at the bottom, and DTU14, Acetomicrobium, and Hydrothermae showing higher RA at the top (Figs. S6 and S8, SM). In addition, Thermoactogenium, not present in the

Table 4ASV taxonomic assignments and their closest relatives determined by NCBI BLAST.

ASV taxonomic assignment	NCBI BLAST analysis	Similarity (%)
Archaea		
Methanothermobacter	Methanothermobacter	100
	thermautotrophicus	
Methanobacterium	Methanobacterium formicicum	100
Methanosarcina	Methanosarcina thermophila	100
Bacteria		
Acetomicrobium	Acetomicrobium mobile	98
Aggregatilineales	Bacterium YC-LK-LKJ3	88
Caldicoprobacter	Caldicoprobacter sp. Acc8	93
Coprothermobacter	Coprothermobacter proteolyticus	100
D8A-2	'Candidatus Syntrophonatronum acetioxidans'	91
Desulfitobacteriaceae	Desulfosporosinus sp. FE18	96
Desulfitibacter	Calderihabitans maritimus strain KKC1	92
DTU014	Koleobacter methoxysyntrophicus	88
Haloplasma	Bacterium ADC-6-1	100
Hydrothermae	Thermotogaless p. SRI-15	96
MBA03	Bacterium ADC-6-6	100
Symbiobacterium	Symbiobacterium thermophilum	100
Syntrophaceticus	Syntrophaceticus schinkii	94
Tepidimicrobium	Tepidimicrobium ferriphilum	93
Thermacetogenium	Thermacetogenium phaeum	99
W5	'Candidatus Cloacamonas acidaminovorans'	89

liquid, appeared only on the carriers at the bottom. This difference between the TBR levels (top, middle and bottom) can be observed in Fig. 5b, where the separation along the first principal component (34 % variance) indicates the difference in the carrier biofilm bacterial community for day 564 (NMSR-trial) and day 666 (liquid recirculation trial), respectively. However, the bacterial community in the TBR liquid on the corresponding days only shows minor differences with the carriers along the second principal component (19 % variance).

4. Discussion

4.1. The effect of nutrient medium supply rate on syngas biomethanation

Recent studies have demonstrated that digestates can serve as viable substitutes for defined nutrient media in syngas biomethanation (Andreides et al., 2022; Cheng et al., 2022; Ali et al., 2024; Goonesekera et al., 2024). However, digestates differ significantly in nutrient composition due to variations in origin and treatment, which complicates direct comparison between studies and limits the generalization of results beyond the specific digestate used. Still, digestate from a wellfunctioning biogas process would indicate that nutrients for microbial activity and growth are present in the sufficient concentrations. The definition of nutrient media addition varies among the literature (either as HRT or as addition rate (mL/d), making it difficult to compare the process performances concerning the nutrient medium supply. Therefore, the present study introduced the new parameter presented as Nutrient Medium Supply Rate (NMSR; mL/(Lpbv·d)), which combines the TBR setup (volume of packed bed and volume of liquid in the TBR) with the nutrient medium addition rate (mL/d) and relates them to the total packed bed volume (Lpby).

The present study was performed with NMSRs below the average values reported in the literature (mentioned below), none of which observed nutrient limitations. NMSRs in the literature for continuous TBR syngas biomethanation using digestate as nutrient medium were recalculated based on liquid reservoir volume and HRT and range from 6 to $200 \, \text{mL/(L_{pbv} \cdot d)}$, with corresponding HRTs of $5-31.5 \, \text{days}$ (Andreides et al., 2022; Cheng et al., 2022; Ali et al., 2024; Goonesekera et al., 2024; Gabler et al., 2025). In the present study, NMSRs were between 11 and $22 \, \text{mL/(L_{pbv} \cdot d)}$ (HRT $9-18 \, d$), with conversion rates of H_2 and CO

exceeding 99 %, at an NMSR of 14 mL/(Lpby·d) and an HRT of 14 days. During the assessment of different operation temperatures using a 1 L TBR, Andreides et al. (2022) set the NMSR to 200 mL/(L_{pbv}·d) (HRT 5 d), the highest reported value for continuous TBR syngas biomethanation studies. They achieved H2 and CO conversion rates similar to those observed in our study but with comparably lower MERs of 1.5 and 2.1 L/ (Lpby·d) under mesophilic and thermophilic conditions, respectively. Similarly to the present study, they did not observe limitations in macronutrient concentrations, as no decrease in syngas conversion rates occurred. The syngas load was maintained at 13.5 $L/(L_{pbv}\cdot d)$ throughout their study, and it was assumed that the maximum consumption capacity of the biofilm had not been reached; therefore, the nutrient level was sufficient compared to the demand (Andreides et al., 2022). In line with Andreides et al. (2022), another study for TBR syngas biomethanation reported significantly higher MERs under thermophilic conditions (4.6 L/(Lpbv·d)) compared to mesophilic conditions (1.9 L/ $(L_{pbv} \cdot d)),$ operating a NMSR of 153 mL/(L_{pbv} \cdot d) (HRT 8 d) with a defined nutrient medium (Asimakopoulos et al., 2020). The reported MERs are slightly above those of the present study.

In another study by Ali et al. (2024), where the utilization of CO was assessed as a sole carbon source in a 0.7 L TBR, a NMSR of 41 mL/ (Lpby·d) (HRT 31.5 d) was applied, achieving optimal performance at a GRT of 1 h with an 88 % CO conversion rate. Furthermore, in a study by Goonesekera et al. (2024), an NMSR of 50 mL/(Lpbv·d) (HRT 20 d) was used for a thermophilic 1 L TBR, where process limitations related to syngas composition and mass-transfer conditions were examined. At this NMSR and similar GRT of 1 h compared to the present study, H2 and CO conversion rates ranged approximately between 80-90 % and 40-80 %, respectively, depending on the applied liquid recirculation rate. The addition of trace elements and an increased liquid recirculation rate led to a 59 % increase in CH₄ productivity and full syngas conversion at a GRT of 1 h (Goonesekera et al., 2024). High syngas loads of 27-28 L/ (L_{pbv}·d) (GRT 0.9 h) with high H₂ and CO conversion rates (>99 %) were achieved using an NMSR of 27 mL/($L_{pbv} \cdot d$) (HRT 7.5 d) in a thermophilic 5 L TBR (Gabler et al., 2025). Cheng et al. (2022) observed decreased H2 and CO conversion rates and the corresponding MERs when the NMSR was stepwise decreased from 29 mL/(Lpby·d) to 6 mL/ (Lpbv·d) (HRT 5-25 d) in a mesophilic 35 L TBR. Moreover, low NMSRs were identified to cause declining conversion of H2 and CO (Cheng et al., 2022), which is in line with our results observing reduced conversion rates at an NMSR of 11 mL/(L_{pbv} ·d) under thermophilic conditions. Most efficient syngas biomethanation was observed at a minimum NMSR of 14 mL/ $(L_{\rm phy}\cdot d)$ for the conditions within the present study.

The fast recovery after the standby period from day 494 to 503 illustrates the robustness of TBR biomethanation systems. The microbial community could remain without gaseous substrate over a long period, in line with the results of previous studies on biomethanation of $\rm H_2$ and $\rm CO_2$ (Jønson et al., 2022; Feickert Fenske et al., 2023a). Jønson et al. (2022) were regaining the initial TBR performance within 6–12 h after standby periods between 0.5 and 3 days. Moreover, Feickert Fenske et al. (2023a) observed a fast recovery of a biomethanation process of $\rm H_2$ and $\rm CO_2$, continuously operated in an 800 L pilot-scale TBR, testing standby periods of 14 and 49 days, obtaining $\rm CH_4$ productivity to recover by >96 % within 24 h. The results of the present study suggest that restarting after a standby period should be characterized by comparatively low syngas loads of ca. 20 % of the maximum previously applied syngas loads, followed by stepwise increases of syngas loads considering the observed conversion rates of $\rm H_2$ and $\rm CO$.

The syngas biomethanation performance in the last period (days 522–564), characterized by a NMSR of 14 mL/(L_{pbv} ·d) (HRT of 14.5 d), was lower compared to the periods before the standby period (Fig. 2). Given that the concentration of macronutrients measured in the TBR liquid phase was sufficient, a potential shortage of N, P or S can be excluded. This observation is in line with findings from a previous study, which utilized the same digestate (Gabler et al., 2025). Goonesekera et al. (2024) observed a positive effect on syngas biomethanation due to

trace element supplementation. It might be possible that the consecutive decrease of NMSR from 22 to 11 mL/($L_{\rm pbv}$ -d) before the standby period resulted in the lack of certain trace elements. However, this can only be assumed because the concentrations of, e.g., Fe, Ni, and Co in the liquid phase were not systematically followed. Another possible reason for the reduced reactor performance after day 520 could be the accumulation of solids and sediments in both the reactor liquid and the packed bed. During the periods with lower NMSR, the liquid phase remained longer in the TBR compared to periods of higher nutrient media addition, and less volume, including solids and sediments, was discharged. This could also have resulted in partial clogging within the packed bed, hindering the syngas from reaching all zones of biofilm on the carriers and, thus, leading to a less active reactor volume and lower total gas-liquid mass transfer area.

4.2. The influence of liquid recirculation regimes on syngas biomethanation

Balancing the liquid recirculation related to nutrient supply and gasliquid mass transfer limitations is a key parameter for efficient TBR syngas biomethanation. Lowering the liquid recirculation rate might be associated with potential clogging in TBRs. However, the volatile suspended solids in the TBR liquid are considered to be very low, as reported by Asimakopoulos et al. (2019) (< 0.6 g/L), in comparison to other reactor designs such as CSTR (Figueras et al., 2021) (11 g/L). Our observations during carrier sampling did not indicate any clogging for the TBR setup used. Still, reduced liquid recirculation can improve gasliquid mass transfer, as the liquid thickness on the biofilm is lower (Burkhardt et al., 2015). Similar findings were reported by Sieborg et al. (2021), observing increased H₂ conversion rates at reduced liquid recirculation in TBR biomethanation of H2 and CO2. Among different studies in the literature for syngas biomethanation, the liquid recirculation regimes have been operated both continuously and intermittently (Aryal et al., 2021; Andreides et al., 2022; Ali et al., 2024; Goonesekera et al., 2024; Gabler et al., 2025).

The reduced liquid recirculation, i.e., the lower recirculation frequencies compared to the NMSR sub-trial, resulted in reduced syngas biomethanation performance with lower syngas loads of 19 L/(L_{nbv}·d) (with a corresponding GRT of 1.3 h) and lower MERs of 3.4 L/(Lpbv·d). More specifically, the biological conversion of CO was more affected, whereas the H₂ conversion was more resilient, with conversion rates ranging between 98 and 99 % (Fig. 3). This is consistent with several other studies and highlights that the gas-liquid mass transfer of CO is the major bottleneck for syngas biomethanation due to low CO solubility compared to H₂ (Asimakopoulos et al., 2021; Paniagua et al., 2022). Underlining this, it has been shown that every single recirculation occasion can have an inhibitory influence on the biological conversion of CO (Fig. 4), whereas the H₂ conversion is not as affected, which can be explained by a higher solubility of H2 compared to CO and by the reduced transfer of gaseous substrate into the microbial cells when the liquid covers the biofilm (Sieborg et al., 2021). Similar findings were reported by Jensen et al. (2021) who observed significant declines in H2 conversion rate (99 to 79 %) and CH₄ concentration in the product gas (94 to 67 %) after intermittent recirculation of the liquid phase during biomethanation of H2 and CO2 in a mesophilic 8.3 L TBR. In another study for the biomethanation of H2 and CO2 in a 0.5 L TBR using pasteurized cow manure as nutrient media, Ashraf et al. (2021) found that a 20-fold increase in the nutrient liquid flow rate during continuous recirculation resulted in reduced H2 conversion rate (-9 %) and CH4 productivity (-13.5 %). Here, the authors suspected a change in hydrodynamics, leading to a higher gas-liquid boundary inhibiting the gas from reaching the active biofilm to convert H2 and CO2 into CH4. In opposite, Goonesekera et al. (2024) observed and improved mass transfer and increased conversion rates of (+10 %) and CO (+40 %) due to increased liquid recirculation rate from 20 to 280 mL/min. However, the examined liquid recirculation duration in the present study did not seem to affect the $\rm H_2$ and CO conversion rates, which is reasonable as the average recirculation flow rate of the pump (40 L/h) was constant, likely resulting in a comparable liquid-biofilm boundary section among the different recirculation durations of 20, 40, and 80 s.

An important aspect to consider regarding recirculation regimes in TBR biomethanation is the liquid hold-up capacity of the carrier material. Jensen et al. (2021) compared plastic, cellulosic, and clay-based carriers concerning their liquid hold-up capacity for TBR biomethanation of H2 and CO2. Clay-based carriers are characterized by a high porosity and a similar specific area (550 to 1020 m²/m³), compared to the more commonly used plastic equivalents (300-950 m²/m³), and can hold the liquid to a significantly higher percentage after 30 min (7-14 vol% compared to 1-3 vol% for the plastic and cellulose-based carriers). Based on that, Jensen et al. (2021) selected crushed clay as carrier material for subsequent biogas upgrading trials in a mesophilic 8.3 L TBR while recirculating the liquid phase once per day. Interestingly, the H₂ conversion rate decreased below 70 % after the daily liquid recirculation and did not fully recover within 210 min afterwards. A similar behavior of long recovery time, but for CO conversion only, was found within the present study (Fig. 4). However, the disruptive influence of each recirculation occasion on the H2 and CO conversion rates was not as pronounced as mentioned by Jensen et al. (2021) (Fig. 4). In the present study, the TBR was filled with a high-density polyethylene carrier (AnoxKaldness K1 500) that has a specific surface area of 500 m^2/m^3 , which is within the range of plastic carriers (320–950 m^2/m^3) used in other TBR syngas biomethanation studies (Aryal et al., 2021; Asimakopoulos et al., 2021; Andreides et al., 2022; Cheng et al., 2022; Goonesekera et al., 2024). Plastic carriers have a significantly lower liquid hold-up capacity and, to maintain effective syngas biomethanation, those TBRs utilizing such material need more regular liquid recirculation compared to TBRs with clay-based carriers. Continuous recirculation is not necessary; however, the recirculation regime should be based on the TBR settings, such as the liquid hold-up capacity of the carriers, the applied syngas loads, and the utilized nutrient medium. Thus, for a sufficient nutrient supply to the biofilm, a low recirculation duration of 20 s combined with higher recirculation frequencies (> 48 d⁻¹) can be assumed as a well-balanced condition for our setup.

4.3. Microbial community development

While the process performance experienced some fluctuations, the microbial community did not show any major changes in both sub-trials concerning NMSR and liquid recirculation regime, with only small differences, even during the standby period and the subsequent decreases in the syngas loads (Figs. 4 and S5-S8, SM).

In line with several other studies on thermophilic biomethanation with syngas or H2 and CO2, the dominating methanogenic genus was Methanothermobacter (Porte et al., 2019; Ali et al., 2024; Gabler et al., 2025). This genus can grow with either CO or CO₂ as the sole carbon source and utilize formate and H₂ and CO₂ as the sole energy source at thermophilic temperatures (Diender et al., 2016). In addition, mainly during the NMSR sub-trial, Methanobacterium was present at comparably higher abundance and identified to belong to M. formicicum. Even though this methanogen is a mesophilic species, it has also been found in thermophilic biomethanation (Porte et al., 2019). M. formicicum can utilize H₂/CO₂ and formate as a carbon and energy source (Battumur et al., 2016). Interestingly, during the recirculation regime period, the same ASV for Methanobacterium dropped to below 1 % RA, suggesting a negative effect on this methanogen by decreasing the liquid recirculation frequency. In contrast to Methanothermobacter, members within Methanobacterium have not been previously shown to utilize CO, and thus the decrease of this ASV was likely not linked to the observed reduction in CO conversion. The presence of this methanogen mainly during the NMSR sub-trial might explain the separation of the archaeal community in addition to the correlation with CO and H2 conversion

rates, as seen in Fig. 5a. The *Methanosarcina* ASV observed at higher RA on the top carrier during the NMSR sub-trial was closely identified as *M. thermophila*, an acetate-utilizing species that also may slowly grow on H₂ and CO₂ (Zinder et al., 1985). Members in the genus *Methanosarcina* have been previously recovered in both mesophilic and thermophilic syngas biomethanation processes (Aryal et al., 2021; Goonesekera et al., 2024), several at higher RA on the carriers as compared to liquid, as seen in the present study.

During both phases of the experiment, several fermenting bacteria likely producing acetate and other organic acids were identified. Hydrothermae was abundant in both phases of the experiment. This ASV was closely identified with Thermotogales sp. SRI-15, belonging to the order Thermotogales, is known to include thermophilic fermenting members that produce acetate and H₂/CO₂ (Reysenbach et al., 2001). The type species of Haloplasma (H. contractile) is fermentative and produces lactate. Tepidimicrobium ASV most likely represented another acetate producer (Niu et al., 2009), sharing 93 % similarity with T. ferriphilum. Members of the Caldicoprobacter genus are fermenters that can produce lactate, acetate, ethanol, and H2/CO2 (Yokoyama et al., 2010). Acetomicrobium, more abundant during the liquid recirculation sub-trial, was confirmed by NCBI BLAST to be A. mobile, which is a sugar and organic acid fermenter producing acetate and H2/CO2 (Menes and Muxi, 2002). Coprothermobacter, showing the same pattern, is a proteolytic fermenter producing acetate and H2/CO2 as main products, and its growth has been shown to be enhanced when combined with M. thermautorophicus (Sasaki et al., 2011). Coprothermobacter has been previously described as part of the core bacterial group in thermophilic biomethanation systems (Chen et al., 2021; Sieborg et al., 2025). These fermenting bacteria were likely feeding on organic components available in the digestate nutrient medium and/or on decaying biomass (Sieborg et al., 2025). The increase of Acetomicrobium and Coprothermobacter ASVs coincided with the transition to the liquid recirculation sub-trial, which could link the RA increase with the reduced liquid recirculation frequency.

Furthermore, Acetomicrobium and Coprothermobacter were found with comparably higher RA on the carriers in the top and middle sections of the reactor, closest to the liquid inflow. Another potential acetate producer may belong to the ASV that is assigned as W5, which has been suggested to be a syntrophic propionate degrader producing acetate and H₂ as end products (Dyksma and Gallert, 2019). Interestingly, no known acetogens seem to be present, which mirrors findings in other studies on thermophilic biomethanation processes (Ali et al., 2024; Sieborg et al., 2025). Due to thermodynamic advantages and higher substrate affinity, methanogens can thrive at lower dissolved H2 concentrations, giving them an advantage over acetogens (Wegener Kofoed et al., 2021). However, under some conditions, like low temperatures, elevated H₂ levels, acetogens become more competitive (Liu et al., 2016; Fu et al., 2019; Voelklein et al., 2019). In line with this, acetogens have been found during continuously operated TBR syngas biomethanation under mesophilic conditions (Cheng et al., 2022). Notably, even though acetate most likely was produced, acetoclastic methanogens (Methanosarcina and Methanothrix) were observed only in low RA throughout the NMSR sub-trial. Methanosarchina has some members that, in addition to acetate, can also use H₂/CO₂ and CO (Rother et al., 2007; Luo et al., 2013). Thus, it cannot with certainty be said that this species was using acetate. Methanothrix, on the other hand, can only use acetate. However, more abundant were several known and potential acetateoxidizing bacteria, indicating their importance for acetate consumption. Potential acetate consumers were represented by Syntrophaceticus, Thermacetogenium, Tepidanaerobacter, DTU014, and MBA03. The ASV belonging to known genera were assigned by NCBI BLAST closely to S. schinkii, T. phaeum, and T. syntrophicus. S. schinkii is a known SAOB that has previously been detected in thermophilic biogas processes and described to play a key role in syngas conversion while partnering with Methanothermobacter (Singh et al., 2023; Ali et al., 2024). Tepidanaerobacter is known to have members that are SAOBs, but

T. syntrophicus is described as a syntrophic alcohol- and lactatedegrading bacterium (Sekiguchi et al., 2006; Westerholm et al., 2011). T. phaeum is known to convert acetate in syntrophy with hydrogenotrophic methanogens but can also take on the role of an acetogen by producing acetate by converting H₂ and CO₂ (Hattori et al., 2005), why it is not possible to determine the true role of T. phaeum. Notably, several of these known SAOBs were found on the carriers in the bottom fraction of the reactor, where the inlet of syngas is located with a high partial pressure of H₂. However, SAOBs typically only thrive at very low H₂ partial pressure, i.e., $<10^{-4}$ atm at 35 °C (Lee and Zinder, 1988). The relatively higher abundance of these bacteria on the bottom carriers indicates biofilm formation on the carriers could change the microbial kinetics and provide efficient gas-liquid mass transfer to potentially ensure efficient methanogenic H2 removal to maintain favorable conditions for SAOBs (Stewart, 2003). However, additional investigations of microbial kinetics are required to provide in-depth explanations of the high presence of SAOBs near the gas inlet. The ASVs belonging to DTU014 and MBA03 have also been previously proposed to be potential SAOBs (Kamravamanesh et al., 2023), and additionally, the D8A-2 ASV could represent another acetate oxidizer as the NCBI BLAST analysis identified with the closest known relative to be 'Candidatus Syntrophonatronum acetioxidans', which has been characterized to oxidize acetate in the presence of sulfate-reducing bacteria (SRB) (Sorokin et al., 2014). SRB use the same substrates as methanogens, and some can also use CO as an electron donor (Parshina et al., 2005). In the presence of sulfate, these bacteria are strong competitors with methanogens, and their activity results in H₂S (Dar et al., 2008). The concentration of sulfate in the nutrient medium was between 160 and 320 mg/L throughout the first part of the study until day 564, which was accompanied by H2S levels of mainly 10-60 ppm in the product gas (Fig. S2b, SM), suggesting some activity of sulfate-reducing bacteria. SRBs could have been represented by two ASVs, one belonging to Desulfitobacteriaceae, according to NCBI blast, most closely related to genus Desulfosorinus (Pester et al., 2012), and one belonging to Desulfitibacter (Nielsen et al., 2006), present both in the liquid and on the carriers consistently throughout the study.

5. Conclusions

Nutrient medium supply rate (NMSR) and liquid recirculation regimes were assessed for continuous biomethanation of syngas (40 % $\rm H_2$, 30 % CO, 20 % CO₂, 10 % N₂) in a thermophilic 5 L TBR, using polyethylene carrier material and diluted digestate for nutrient supply. Over time, the reduced nutrient supply rate resulted in a slow decline of $\rm H_2$ and CO conversion rates, especially of CO. At a minimum NMSR of 14 mL/(Lpbv·d), high $\rm H_2$ and CO conversion rates (>99 %) were achieved with a corresponding maximum methane evolution rate (MER) of 4.3 L/(Lpbv·d) at a gas retention time of 1 h. Intermittent liquid recirculation for efficient syngas biomethanation was studied, applying different frequencies and durations. At reduced recirculation frequencies, the biological syngas conversion deteriorated, leading to a maximum MER of 3.4 L/(Lpbv·d), whereas the recirculation duration per se did not influence the syngas biomethanation performance.

The microbial community profile in the TBR showed similar structures throughout the different operational phases, with only small differences, and the community was also similar between the carrier and liquid. Thus, the observed differences in process performance were likely caused by differences in activity and not community structure or methanogenic abundance. The syngas converting community was mainly composed of the hydrogenotrophic methanogen *Methanothermobacter*, with the ability to consume both H₂/CO₂ and CO, and different syntrophic acetate-oxidizing bacteria, such as *Syntrophaceticus* and *Thermacetogenium*. In addition, different heterotrophic fermentative bacteria were present, likely to feed on organic carbon in the nutrient medium or cell debris.

CRediT authorship contribution statement

Florian Gabler: Writing – original draft, Visualization, Formal analysis, Data curation, Conceptualization. George Cheng: Writing – review & editing, Visualization, Formal analysis, Data curation. Leticia Pizzul: Writing – review & editing, Visualization, Supervision, Funding acquisition, Conceptualization. Anna Schnürer: Writing – review & editing, Supervision, Funding acquisition, Conceptualization. Åke Nordberg: Writing – review & editing, Supervision, Funding acquisition, Conceptualization.

Declaration of competing interest

The authors declare that they have no known competing financial interests or personal relationships that could have appeared to influence the work reported in this paper.

Acknowledgments

This project was funded by the Swedish Energy Agency [149656-1] and Formas (2018-01341). The authors acknowledge Vasiliki Tsamadou for assistance with DNA extraction.

Appendix A. Supplementary data

Supplementary data to this article can be found online at https://doi.org/10.1016/j.biteb.2025.102353.

Data availability

The sequence data generated and analyzed from this study are made available in the NCBI repository in BioProject PRJNA1276488.

References

- Ali, R., Samadi, H., Yde, L., Ashraf, M.T., 2024. Carbon monoxide conversion by anaerobic microbiome in a thermophilic trickle bed reactor. Biochem. Eng. J. 212.
- Andreides, D., Stransky, D., Bartackova, J., Pokorna, D., Zabranska, J., 2022. Syngas biomethanation in countercurrent flow trickle-bed reactor operated under different temperature conditions. Renew. Energy 199, 1329–1335. https://doi.org/10.1016/j. renews. 2022.09.072
- Aryal, N., Odde, M., Petersen, C.B., Ottosen, L.D.M., Kofoed, M.V.W., 2021. Methane production from syngas using a trickle-bed reactor setup. Bioresour. Technol. 333. https://doi.org/10.1016/j.biortech.2021.125183. ARTN 125183.
- Ashraf, M.T., Yde, L., Triolo, J.M., Wenzel, H., 2021. Optimizing the dosing and trickling of nutrient media for thermophilic biomethanation in a biotrickling filter. Biochem. Eng. J. 176. https://doi.org/10.1016/j.bej.2021.108220.
- Asimakopoulos, K., Gavala, H.N., Skiadas, I.V., 2019. Biomethanation of syngas by enriched mixed anaerobic consortia in trickle bed reactors. Waste Biomass Valoriz. 11 (2), 495–512. https://doi.org/10.1007/s12649-019-00649-2.
- Asimakopoulos, K., Łeżyk, M., Grimalt-Alemany, A., Melas, A., Wen, Z., Gavala, H.N., Skiadas, I.V., 2020. Temperature effects on syngas biomethanation performed in a trickle bed reactor. Chem. Eng. J. 393. https://doi.org/10.1016/j.cej.2020.124739.
- Asimakopoulos, K., Kaufmann-Elfang, M., Lundholm-Høffner, C., Rasmussen, N.B.K., Grimalt-Alemany, A., Gavala, H.N., Skiadas, I.V., 2021. Scale up study of a thermophilic trickle bed reactor performing syngas biomethanation. Appl. Energy 290. https://doi.org/10.1016/j.apenergy.2021.116771.
- Battumur, U., Yoon, Y.-M., Kim, C.-H., 2016. Isolation and characterization of a new Methanobacterium formicicum KOR-1 from an anaerobic digester using pig slurry. Asian Australas. J. Anim. Sci. 29 (4), 586–593. https://doi.org/10.5713/ aias.15.0507.
- Bilgic, B., Andersen, T.O., Abera, G.B., Sposób, M., Feng, L., Horn, S.J., 2025. Syngas biomethanation using trickle bed reactor, impact of external hydrogen addition at high loading rate. Bioresour. Technol. Rep. https://doi.org/10.1016/j. bireb.2025.102197.
- Burkhardt, M., Koschack, T., Busch, G., 2015. Biocatalytic methanation of hydrogen and carbon dioxide in an anaerobic three-phase system. Bioresour. Technol. 178, 330–333. https://doi.org/10.1016/j.biortech.2014.08.023.
- Chen, L., Du, S., Xie, L., 2021. Effects of pH on ex-situ biomethanation with hydrogenotrophic methanogens under thermophilic and extreme-thermophilic conditions. J. Biosci. Bioeng. 131 (2), 168–175. https://doi.org/10.1016/j.ibiosc.2020.09.018.
- Cheng, G., Gabler, F., Pizzul, L., Olsson, H., Nordberg, A., Schnurer, A., 2022. Microbial community development during syngas methanation in a trickle bed reactor with

- various nutrient sources. Appl. Microbiol. Biotechnol. 106 (13–16), 5317–5333. https://doi.org/10.1007/s00253-022-12035-5.
- Dar, S.A., Kleerebezem, R., Stams, A.J., Kuenen, J.G., Muyzer, G., 2008. Competition and coexistence of sulfate-reducing bacteria, acetogens and methanogens in a lab-scale anaerobic bioreactor as affected by changing substrate to sulfate ratio. Appl. Microbiol. Biotechnol. 78 (6), 1045–1055. https://doi.org/10.1007/s00253-008-1301-8
- Diender, M., Pereira, R., Wessels, H.J., Stams, A.J., Sousa, D.Z., 2016. Proteomic analysis of the hydrogen and carbon monoxide metabolism of *Methanothermobacter marburgensis*. Front. Microbiol. 7, 1049. https://doi.org/10.3389/fmicb.2016.01049.
- Dyksma, S., Gallert, C., 2019. Candidatus Syntrophosphaera thermopropionivorans: a novel player in syntrophic propionate oxidation during anaerobic digestion. Environ. Microbiol. Rep. 11 (4), 558–570. https://doi.org/10.1111/1758-2229.12759.
- Feickert Fenske, C., Kirzeder, F., Strubing, D., Koch, K., 2023a. Biogas upgrading in a pilot-scale trickle bed reactor - long-term biological methanation under real application conditions. Bioresour. Technol. 376, 128868. https://doi.org/10.1016/j. biortech.2023.128868.
- Feickert Fenske, C., Strubing, D., Koch, K., 2023b. Biological methanation in trickle bed reactors - a critical review. Bioresour. Technol. 385, 129383. https://doi.org/ 10.1016/j.biortech.2023.129383.
- Figueras, J., Benbelkacem, H., Dumas, C., Buffiere, P., 2021. Biomethanation of syngas by enriched mixed anaerobic consortium in pressurized agitated column. Bioresour. Technol. 338, 125548. https://doi.org/10.1016/j.biortech.2021.125548.
- Fu, B., Jin, X., Conrad, R., Liu, H., Liu, H., 2019. Competition between chemolithotrophic acetogenesis and hydrogenotrophic methanogenesis for exogenous H2/CO2 in anaerobically digested sludge: impact of temperature. Front. Microbiol. 10, 2418. https://doi.org/10.3389/fmicb.2019.02418.
- Gabler, F., Cheng, G., Pizzul, L., Schnürer, A., Nordberg, Å., 2025. Comparative evaluation of digestate and reject water as nutrient media for syngas biomethanation in thermophilic trickle-bed reactors. Bioresour. Technol. 435. https://doi.org/ 10.1016/j.biortech.2025.132893.
- Goonesekera, E.M., Grimalt-Alemany, A., Thanasoula, E., Yousif, H.F., Krarup, S.L., Valerin, M.C., Angelidaki, I., 2024. Biofilm mass transfer and thermodynamic constraints shape biofilm in trickle bed reactor syngas biomethanation. Chem. Eng. J. 500. https://doi.org/10.1016/j.cej.2024.156629.
- Grimalt-Alemany, A., Skiadas, I.V., Gavala, H.N., 2017. Syngas biomethanation: state-of-the-art review and perspectives. Biofuels Bioprod. Biorefin. 12 (1), 139–158. https://doi.org/10.1002/bbb.1826.
- Hattori, S., Galushko, A.S., Kamagata, Y., Schink, B., 2005. Operation of the CO dehydrogenase/acetyl coenzyme a pathway in both acetate oxidation and acetate formation by the syntrophically acetate-oxidizing bacterium Thermacetogenium phaeum. J. Bacteriol. 187 (10), 3471–3476. https://doi.org/10.1128/ JB.187.10.3471-3476.2005.
- Jensen, M.B., Poulsen, S., Jensen, B., Feilberg, A., Kofoed, M.V.W., 2021. Selecting carrier material for efficient biomethanation of industrial biogas-CO2 in a trickle-bed reactor. J CO: Util 51, 101611. https://doi.org/10.1016/j.icou.2021.101611.
- Jønson, B.D., Tsapekos, P., Tahir Ashraf, M., Jeppesen, M., Ejbye Schmidt, J., Bastidas-Oyanedel, J.R., 2022. Pilot-scale study of biomethanation in biological trickle bed reactors converting impure CO(2) from a full-scale biogas plant. Bioresour. Technol. 365. 128160. https://doi.org/10.1016/j.biortech.2022.128160.
- Kamravamanesh, D., Rinta Kanto, J.M., Ali-Loytty, H., Myllärinen, A., Saalasti, M., Rintala, J., Kokko, M., 2023. Ex-situ biological hydrogen methanation in trickle bed reactors: Integration into biogas production facilities. Chem. Eng. Sci. 269. https:// doi.org/10.1016/j.ces.2023.118498.
- Larsson, A., Gunnarsson, I., tengberg, F., 2019. The GoBiGas Project Demonstration of the Production of Biomethane from Biomas Via Gasification. AB, G.E.
- Lee, M.J., Zinder, S.H., 1988. Hydrogen partial pressures in a thermophilic acetate-oxidizing methanogenic coculture. Appl. Environ. Microbiol. 54 (6), 1457–1461. https://doi.org/10.1128/aem.54.6.1457-1461.1988.
- Liu, R., Hao, X., Wei, J., 2016. Function of homoacetogenesis on the heterotrophic methane production with exogenous H2/CO2 involved. Chem. Eng. J. 284, 1196–1203. https://doi.org/10.1016/j.cej.2015.09.081.
- Luo, G., Wang, W., Angelidaki, I., 2013. Anaerobic digestion for simultaneous sewage sludge treatment and CO biomethanation: process performance and microbial ecology. Environ. Sci. Technol. 47 (18), 10685–10693. https://doi.org/10.1021/ es401018d.
- Menes, R.J., Muxi, L., 2002. Anaerobaculum mobile sp. nov., a novel anaerobic, moderately thermophilic, peptidefermenting bacterium that uses crotonate as an electron acceptor, and emended description of the genus Anaerobaculum. Int. J. Syst. Evol. Microbiol. 52, 157–164. https://doi.org/10.1099/00207713-52-1-157.
- Evol. Microbiol. 52, 157–164. https://doi.org/10.1099/00207713-52-1-157.

 Neto, A.S., Wainaina, S., Chandolias, K., Piatek, P., Taherzadeh, M.J., 2025. Exploring the potential of syngas fermentation for recovery of high-value resources: a comprehensive review. Curr. Pollut. Rep. 11 (1), 7. https://doi.org/10.1007/s40726-074-00337-3
- Nielsen, M.B., Kjeldsen, K.U., Ingvorsen, K., 2006. Desulfitibacter alkalitolerans gen. nov., sp. nov., an anaerobic, alkalitolerant, sulfite-reducing bacterium isolated from a district heating plant. Int. J. Syst. Evol. Microbiol. 56 (Pt 12), 2831–2836. https://doi.org/10.1098/iis.0.64356.0
- Niu, L., Song, L., Liu, X., Dong, X., 2009. Tepidimicrobium xylanilyticum sp. nov., an anaerobic xylanolytic bacterium, and emended description of the genus Tepidimicrobium. Int. J. Syst. Evol. Microbiol. 59 (Pt 11), 2698–2701. https://doi. org/10.1099/ijs.0.005124-0.
- Paniagua, S., Lebrero, R., Munoz, R., 2022. Syngas biomethanation: current state and future perspectives. Bioresour. Technol. 358, 127436. https://doi.org/10.1016/j. biortech.2022.127436.

- Parshina, S.N., Kijlstra, S., Henstra, A.M., Sipma, J., Plugge, C.M., Stams, A.J., 2005. Carbon monoxide conversion by thermophilic sulfate-reducing bacteria in pure culture and in co-culture with Carboxydothermus hydrogenoformans. Appl. Microbiol. Biotechnol. 68 (3), 390–396. https://doi.org/10.1007/s00253-004-1878-
- Pester, M., Brambilla, E., Alazard, D., Rattei, T., Weinmaier, T., Han, J., Lucas, S., Lapidus, A., Cheng, J.F., Goodwin, L., Pitluck, S., Peters, L., Ovchinnikova, G., Teshima, H., Detter, J.C., Han, C.S., Tapia, R., Land, M.L., Hauser, L., Kyrpides, N.C., Ivanova, N.N., Pagani, I., Huntmann, M., Wei, C.L., Davenport, K.W., Daligault, H., Chain, P.S., Chen, A., Mavromatis, K., Markowitz, V., Szeto, E., Mikhailova, N., Pati, A., Wagner, M., Woyke, T., Ollivier, B., Klenk, H.P., Spring, S., Loy, A., 2012. Complete genome sequences of *Desulfosporosinus orientis* DSM765T, *Desulfosporosinus youngiae* DSM17734T, *Desulfosporosinus meridiei* DSM13257T, and *Desulfosporosinus acidiphilus* DSM22704T. J. Bacteriol. 194 (22), 6300–6301. https://doi.org/10.1128/JB.01392-12
- Porte, H., Kougias, P.G., Alfaro, N., Treu, L., Campanaro, S., Angelidaki, I., 2019. Process performance and microbial community structure in thermophilic trickling biofilter reactors for biogas upgrading. Sci. Total Environ. 655, 529–538. https://doi.org/ 10.1016/j.scitotenv.2018.11.289.
- Ren, J., Liu, Y.-L., Zhao, X.-Y., Cao, J.-P., 2020. Methanation of syngas from biomass gasification: an overview. Int. J. Hydrog. Energy 45 (7), 4223–4243. https://doi.org/ 10.1016/j.ijhydene.2019.12.023.
- Reysenbach, A.-L., Huber, R., Stetter, K.O., Davey, M.E., MacGregor, B.J., Stahl, D.A., 2001. Phylum BII. Thermotogae phy. nov. In: Boone, D.R., Castenholz, R.W., Garrity, G.M. (Eds.), Bergey's Manual® of Systematic Bacteriology: Volume One: The Archaea and the Deeply Branching and Phototrophic Bacteria. Springer New York, New York, NY, pp. 369–387. https://doi.org/10.1007/978-0-387-21609-6_19.
- Rother, M., Oelgeschlager, E., Metcalf, W.M., 2007. Genetic and proteomic analyses of CO utilization by *Methanosarcina acetivorans*. Arch. Microbiol. 188 (5), 463–472. https://doi.org/10.1007/s00203-007-0266-1.
- Sancho Navarro, S., Cimpoia, R., Bruant, G., Guiot, S.R., 2016. Biomethanation of syngas using anaerobic sludge: shift in the catabolic routes with the CO partial pressure increase. Front. Microbiol. 7, 1188. https://doi.org/10.3389/fmicb.2016.01188.
- Sasaki, K., Morita, M., Sasaki, D., Nagaoka, J., Matsumoto, N., Ohmura, N., Shinozaki, H., 2011. Syntrophic degradation of proteinaceous materials by the thermophilic strains Coprothermobacter proteolyticus and Methanothermobacter thermautotrophicus. J. Biosci. Bioeng. 112 (5), 469–472. https://doi.org/10.1016/j.jbiosc.2011.07.003.
- Sekiguchi, Y., Imachi, H., Susilorukmi, A., Muramatsu, M., Ohashi, A., Harada, H., Hanada, S., Kamagata, Y., 2006. Tepidanaerobacter syntrophicus gen. nov., sp. nov., an anaerobic, moderately thermophilic, syntrophic alcohol- and lactate-degrading bacterium isolated from thermophilic digested sludges. Int. J. Syst. Evol. Microbiol. 56 (Pt 7), 1621–1629. https://doi.org/10.1099/ijs.0.64112-0.

- Sieborg, M.U., Jensen, M.B., Jensen, B., Kofoed, M.V.W., 2021. Effect of minimizing carrier irrigation on H2 conversion in trickle bed reactors during ex situ biomethanation. Bioresour. Technol. Rep. 16. https://doi.org/10.1016/j. biteb 2021 100876
- Sieborg, M.U., Engelbrecht, N., Singh, A., Schnürer, A., Mørck Ottosen, L.D., Wegener Kofoed, M.V., 2025. Unraveling the effects of temperature on mass transfer and microbiology in thermophilic and extreme thermophilic trickle bed biomethanation reactors. Chem. Eng. J. https://doi.org/10.1016/j.cej.2025.161179.
- Singh, A., Schnurer, A., Dolfing, J., Westerholm, M., 2023. Syntrophic entanglements for propionate and acetate oxidation under thermophilic and high-ammonia conditions. ISME J. 17 (11), 1966–1978. https://doi.org/10.1038/s41396-023-01504-y.
- Sipma, J., Lens, P.N.L., Stams, A.J.M., Lettinga, G., 2003. Carbon monoxide conversion by anaerobic bioreactor sludges. FEMS Microbiol. Ecol. 44 (2), 271–277. https://doi. org/10.1016/S0168-6496(03)00033-3.
- Sorokin, D.Y., Abbas, B., Tourova, T.P., Bumazhkin, B.K., Kolganova, T.V., Muyzer, G., 2014. Sulfate-dependent acetate oxidation under extremely natron-alkaline conditions by syntrophic associations from hypersaline soda lakes. Microbiology (Reading) 160 (Pt 4), 723–732. https://doi.org/10.1099/mic.0.075093-0.
- Stewart, P.S., 2003. Diffusion in biofilms. J. Bacteriol. 185 (5), 1485–1491. https://doi. org/10.1128/jb.185.5.1485-1491.2003.
- Voelklein, M.A., Rusmanis, D., Murphy, J.D., 2019. Biological methanation: strategies for in-situ and ex-situ upgrading in anaerobic digestion. Appl. Energy 235, 1061–1071. https://doi.org/10.1016/j.apenergy.2018.11.006.
- Wegener Kofoed, M.V., Jensen, M.B., Mørck Ottosen, L.D., 2021. Biological upgrading of biogas through CO2 conversion to CH4. In: Emerging Technologies and Biological Systems for Biogas Upgrading, pp. 321–362. https://doi.org/10.1016/b978-0-12-822808-1.00012-x.
- Westerholm, M., Roos, S., Schnurer, A., 2011. Tepidanaerobacter acetatoxydans sp. nov., an anaerobic, syntrophic acetate-oxidizing bacterium isolated from two ammonium-enriched mesophilic methanogenic processes. Syst. Appl. Microbiol. 34 (4), 260–266. https://doi.org/10.1016/j.syapm.2010.11.018.
- Westerholm, M., Isaksson, S., Karlsson Lindsjö, O., Schnürer, A., 2018. Microbial community adaptability to altered temperature conditions determines the potential for process optimisation in biogas production. Appl. Energy 226, 838–848. https:// doi.org/10.1016/j.apenergy.2018.06.045.
- Yokoyama, H., Wagner, I.D., Wiegel, J., 2010. Caldicoprobacter oshimai gen. nov., sp. nov., an anaerobic, xylanolytic, extremely thermophilic bacterium isolated from sheep faeces, and proposal of Caldicoprobacteraceae fam. nov. Int. J. Syst. Evol. Microbiol. 60 (Pt 1), 67–71. https://doi.org/10.1099/ijs.0.011379-0.
- Zinder, S.H., Sowers, K.R., Ferry, J.G., 1985. *Methanosarcina thermophila* sp. nov., a thermophilic, acetotrophic, methane-producing bacterium free. Int. J. Syst. Bacteriol. 35 (4), 522–523. https://doi.org/10.1099/00207713-35-4-522.